

---

# Evaluating Perceptual Distance Models by Fitting Binomial Distributions to Two-Alternative Forced Choice Data

---

Alexander Hepburn<sup>1</sup> Raul Santos-Rodriguez<sup>1</sup> Javier Portilla<sup>2</sup>

## Abstract

Two-alternative forced choice (2AFC) experiments are popular in the visual perception literature to understand how human observers perceive distances within triplets made of a reference image and two distorted versions. Previously, this had been conducted in controlled environments, with triplets sharing images, making it possible to rank the perceived quality and evaluate perceptual distance models against the ranking. Recently, crowd-sourced perceptual datasets have emerged, with no images shared between triplets, making ranking infeasible. Evaluations using this data reduces the judgements on a triplet to a binary decision, namely, whether the distance model agrees with the human decision - which is suboptimal and prone to misleading conclusions. Instead, we statistically model the underlying decision-making process during 2AFC experiments using a binomial distribution. We estimate a smooth and consistent distribution of the judgements on the reference-distorted distance plane, according to each distance model. We estimate the parameter of the local binomial distribution using maximum likelihood, and a global measurement of the expected log-likelihood of the judgements. We calculate meaningful and well-founded metrics, beyond the mere prediction accuracy as percentage agreement and compare to a neural network counterpart, also optimised to maximise likelihood according to a binomial model.

## 1. Introduction

The fundamental problem of replicating the ability of the human visual system to compare images is increasingly important in computer vision. Many *perceptual distance*

*models* have attempted to capture the behaviour of the visual system, whether through extracting and comparing structures present in images (Wang et al., 2004; 2003), modelling mechanisms that are present in the visual pathway (Laparra et al., 2016; Hepburn et al., 2020), or more recently using neural networks pre-trained for classification to extract image features (Zhang et al., 2018; Ding et al., 2020).

The usual paradigm is to obtain a distance replicating human judgements on a dataset gathered through psychophysical experiments. In many datasets, those experiments consist of performing two-alternative forced choice (2AFC), where participants are presented with a triplet of a reference image and two distorted versions of that image (Fechner, 1948). The human observer is then asked to determine which distorted image is perceptually closer to the original. Often, these judgments are then transformed into a mean opinion score (MOS), which is then used to order the distorted images according to the perceived similarity to the corresponding reference (Ponomarenko et al., 2009; 2013; Sheikh et al., 2005; Larson & Chandler, 2010). This requires carefully selecting which images are shown to a given observer, and that there are common images between experiments. Additionally, a distance model can be learned by assuming some distribution and estimating the parameters of the “internal score” a human observer assigns to a given image (Thurstone, 1994).

Traditional perceptual datasets are collected in controlled environments, where variables such as the monitor, distance to screen and environmental lighting are managed. This results in a small but trustable set of measurements. Recently, practitioners have dropped those constraints in favour of more reference images and a larger number of distortions. The Berkeley Adobe Perceptual Patch Similarity (BAPPS) (Zhang et al., 2018) contains judgements of 187,700 image patches using 425 distortions, compared to TID2013 (Ponomarenko et al., 2013) with 25 reference images and 24 distortions. BAPPS contains the raw perceptual judgements, as opposed to only the MOS, as it is infeasible to compute a ranking using triplets that do not share images (Tsukida et al., 2011). From this crowd-sourced data, neural networks have been optimised to maximise the agreement with human observers, in order to create a perceptual distance model (Zhang et al., 2018). However, evaluating

<sup>1</sup>University of Bristol, Bristol, United Kingdom  
<sup>2</sup>Consejo Superior de Investigaciones Científicas (CSIC), Madrid, Spain. Correspondence to: Alexander Hepburn <alex.hepburn@bristol.ac.uk>.

perceptual distance models using such data is non-trivial, as a mapping from the distances between the two distorted images and reference, to the proportion of people that judged the first distorted image closer to the reference, needs to be learnt. The CLIC dataset (Toderici et al., 2021) also releases raw perceptual judgements, although with a varying number of judgements per triplet. Datasets containing only the MOS for each given reference-distorted image pair are also missing some key information, such as the number of human participant judgements per image triplet which can be used to infer uncertainty over the judgement.

Many simplifications and added assumptions are necessary to estimate the distance between images from the 2AFC tests, with different people with unknown response parameters governing their “internal scores” (Thurstone, 1994). However, it is important to note that, for the problem at hand, *we are not interested in estimating the perceived distance between test images presented to subjects*. Instead, we want to objectively evaluate how well different perceptual distance *models* explain the observed 2AFC data.

We follow relevant literature and model the perceptual judgements using a binomial distribution (Thurstone, 1994). We then compute the two distances between images within a triplet using a set of perceptual distance models. We estimate the density of each score given these distances, including smoothing using Gaussian kernels, and fit a binomial model that maximises the likelihood of the judgements. Evaluation metrics such as the likelihood of a judgement according to the binomial model are simple to compute, and can explicitly account for a different number of human judgements used in the experiment, even for individual triplets. Fitting of this model requires little computation and can be easily parallelised. We compare with a simple neural network architecture, optimised to maximise the likelihood of judgements, adhering to the binomial model. The proposed density estimation achieves similar performance whilst using an order of magnitude less parameters and training time, and avoiding overconfidence in regions that lack data.

## 2. Related Work

### 2.1. Perceptual Experiments

Perceptual experiments are performed using a number of methodologies, that differ in both the way the stimuli are presented, and the interaction the participant has with the experiment. We focus on the 2AFC experimental setup, used by popular datasets such as TID 2008 & 2013 (Ponomarenko et al., 2009; 2013) and BAPPS (Zhang et al., 2018). However, TID and other datasets use 2AFC experiments to *rank* distorted images, where the MOS is then calculated and only this is released. BAPPS however presents *random*

triplets to observers and releases the 2AFC judgements. The CLIC dataset (Toderici et al., 2021) also releases the 2AFC judgements, however triplets have a variable number of judgements. An overview of the available visual perception datasets can be found in Appendix A.

Evaluating a perceptual distance model using the MOS is simple. One can simply compute the distance between each reference-distorted pair according to the model, and calculate the correlation between these distances and the MOS. However, with datasets like BAPPS, this is not possible. One evaluation metric is to force the decision to be binary: *according to the distance model, is the first distorted image closer to the reference than the second?* This ignores the number of judgements performed per triplet, wrongly equating a unanimous decision to one that is close to a tie.

(Zhang et al., 2018) address this by transforming the two distances to the proportion of human observers that would judge the first distorted image closer to the reference. This is a non-linear transform that is parameterised by a simple neural network, and optimised to minimise the cross-entropy loss between the output and the 2AFC experimental results. This also allows a parametrisation of a perceptual distance model to be optimised to minimise the cross-entropy loss. However, this is not truly modelling the decision process, and the evaluation consists of calculating the percentage of agreement between the network and human observer. Additionally, to compare different perceptual distances using BAPPS fairly, one would need to fit a separate neural network per distance.

Our proposed method assumes we have access to 2AFC experimental results, although it generalises to any alternative forced choice experiments such as the method of quadruples (Kingdom & Prins, 2010). We focus on BAPPS, as there is also no relationship between triplets (no ranking), which is what the proposed method is designed for. We also report results on the CLIC dataset, where there is a variable number of judgements per triplet.

### 2.2. Perceptual Distances

In traditional perceptual literature, perceptual distances are hand-designed models inspired by findings in vision science. Distances such as SSIM (Wang et al., 2004) and MS-SSIM (Wang et al., 2003) rely on the *structural similarity* between two images, i.e. how do humans perceive structure in an image. Separately, there are distances based on the *visibility of errors*; differences between a reference and distorted image directly impact the similarity. Models using this principle usually transform images to a more “perceptual” space and there compute a Euclidean distance. In the normalised Laplacian pyramid distance (NLPD) (Laparra et al., 2016), such transformations are learned based on reducing redundancy in neighbouring pixels.

More recently, neural networks have been used to extract useful features for perceptual judgements. The Learned Perceptual Image Patch Similarity (LPIPS) (Zhang et al., 2018) uses features extracted from image classification networks, and learns a weighted average of the features that correlates well with human perception. A neural network is then optimised to minimise the cross-entropy with 2AFC data. Although this successfully predicts perception, it lacks underlying assumptions on the psychophysical model that dictates human behaviour in 2AFC experiments. It is also unable to calculate the likelihood of a certain judgement. Deep Image Structure and Texture Similarity (DISTS) builds upon this to include a measure of texture similarity (Ding et al., 2020). The Perceptual Information Metric (PIM) (Bhardwaj et al., 2020) finds a representation that maximises the mutual information between adjacent frames in videos. This representation is then used to compute distances.

For our candidate distances, which we wish to evaluate using the proposed method, we select a variety of traditional and deep learning-based metrics: Euclidean distance, NLPD (Laparra et al., 2016), SSIM (Wang et al., 2004), PIM (Bhardwaj et al., 2020), LPIPS (Zhang et al., 2018) and DISTS (Ding et al., 2020).

### 2.3. Bayesian approach to vision

Maximum likelihood difference scaling (MLDS) (Maloney & Yang, 2003) models the observers ordering and fits a function to predict human perception in difference scales - the perceived difference between stimuli with a particular distortion, or particular direction in image space. The scales are optimised to maximise the likelihood of the human judgements belonging to the scales, assuming a Gaussian distribution. This allows the fitting of continuous functions defined by the practitioner and can be used to estimate the difference scales in continuous physical measurements such as luminance and contrast.

Assuming that a stimuli’s quality can be modelled as a Gaussian random variable, Thurstone proposed different settings depending on the assumptions made on the underlying psychometrics (Thurstone, 1994). The parameters of the Gaussian random variables can be estimated by maximising the likelihood of a set of judgements belonging to a binomial distribution (Tsukida et al., 2011; Silverstein & Farrell, 2001; Jogan & Stocker, 2014), where the means relate to a *scale difference*, given an internal model within each participant.

Unlike the classical problem above, we do not need to rely on any assumed internal response model; we model the discrete decision process itself in the 2AFC tests. We apply a generic and simple random model, the binomial distribution, having as a single parameter the probability of choosing one option vs. the other. This, together with the structure of our

problem, which associates one candidate distance measurement to 2AFC tests, allows us to estimate the probability of choosing one distorted image over the other, for any number of experimental judgements. As a result, we can reliably estimate the fitness of every candidate perceptual distance model in a conceptually and computationally simple way, without adhering to model assumptions about subjective responses.

## 3. Method

Let us consider psychophysical data from 2AFC experiments between two degraded images and a reference image that are presented to the subjects (Ponomarenko et al., 2009; 2013; Zhang et al., 2018; Toderici et al., 2021). We assume  $T$  triplets of images, where each presented triplet  $t$ ,  $(\mathbf{x}_{ref}(t), \mathbf{x}_0(t), \mathbf{x}_1(t))$ , receives a fixed number  $M$  of responses. We define  $n(t) \in [0, M]$  as the number of times  $\mathbf{x}_1(t)$  is deemed to be more similar to  $\mathbf{x}_{ref}(t)$  than  $\mathbf{x}_0(t)$  according to the observer. We propose that these choices are modelled by a binomial distribution  $n \sim \mathcal{B}(M, P)$ , where  $P$  denotes the probability of  $\mathbf{x}_1$  being chosen.

The underlying hypothesis is that there is a perceptual distance model  $d$  that maps two images to their corresponding visual distance, such that the choice count  $n$  is conditionally independent of  $\{\mathbf{x}_{ref}, \mathbf{x}_0, \mathbf{x}_1\}$  given  $(d(\mathbf{x}_{ref}, \mathbf{x}_0), d(\mathbf{x}_{ref}, \mathbf{x}_1))$ . We also define the distance between the reference and first distorted as  $d_0(t) = d(\mathbf{x}_{ref}(t), \mathbf{x}_0(t))$  and distance between the reference and second distorted as  $d_1(t) = d(\mathbf{x}_{ref}(t), \mathbf{x}_1(t))$ . Under the assumed binomial choice model, the previous hypothesis is equivalent to stating that there is a function  $f$ , such that the binomial parameter  $P$  controlling the probability of the choice is  $P(\mathbf{x}_{ref}, \mathbf{x}_0, \mathbf{x}_1) = f(d_0, d_1)$ .

We will refer to the function  $f$  as  $P(d_0, d_1)$  for simplicity, and the parameter corresponding to a particular triplet as  $P(d_0(t), d_1(t))$ . Given a set of psychophysical data corresponding to the previous experimental setup and a perceptual distance model  $d$ , here we address the problem of measuring *how well that candidate function fits the empirical data under the assumed binomial process*. At this point, it is important to note that we should not choose  $P(d_0(t), d_1(t))$  simply as its most likely value  $(n(t)/M)$  according to that particular triplet  $t$ . Instead, due to the noise in the decision process, we must consider other triplet results in the neighbourhood to obtain a smooth and consistent  $P(d_0, d_1)$  function on the whole  $(d_0, d_1)$  distance plane. The reliability of  $P(d_0, d_1)$  critically depends on having a large set of results providing a dense sampling of the  $(d_0, d_1)$  plane.

### 3.1. Maximum-likelihood density estimation

We estimate the empirical densities  $\{p(j, d_0, d_1), j = 1 \dots M\}$ , which model how likely are the events  $\{(d_0, d_1), n = j\}$ . As explained before, to obtain a continuous probability density function (PDF) from a set of discrete events, we use a Gaussian kernel integrating the corresponding samples on the distance plane. This is done separately for each  $j$ , ensuring that  $\int p(j, d_0, d_1), dd_0 dd_1 = P(j) = 1/T \sum \delta(n(t) - j)$ . Then, we compute the overall density on the distance plane as  $p(d_0, d_1) = \sum_{j=1}^M p(j, d_0, d_1)$ . (Note that we can take advantage of the symmetry  $p(d_0, d_1) = p(d_1, d_0)$ , by enforcing it.) Now we can estimate the conditional probabilities

$$Pr(n = j|d_0, d_1) = \frac{p(j, d_0, d_1)}{p(d_0, d_1)}, j = 1 \dots M. \quad (1)$$

In practice, to ensure coverage of the whole  $(d_0, d_1)$  plane in  $[0, 1]$ , we first marginally uniformise the training data (details in Appendix B). To obtain a smooth PDF estimation from a set of discrete points on the  $(d_0, d_1)$  plane, we define a grid made up of evenly spaced points, for which we will estimate the conditional probabilities. Gaussian kernels of a suitable size, centered at each of the discrete points in the training set and evaluated on the grid, are then summed. This is applied separately to each of the sets  $\{(d_0, d_1), n = j\}$ , thus obtaining estimations of  $p(j, d_0, d_1)$  for all  $j$ s. Finally, we compute their sum ( $p(d_0, d_1)$ ) and apply Eq. 1 to obtain the estimated conditional probabilities,  $Pr(n = j|d_0, d_1)$ . According to the assumed model,  $n(t) \sim \mathcal{B}(M, P(d_0(t), d_1(t)))$ , we know the theoretical binomial probability of each  $n$  as a function of  $P(d_0, d_1)$  and  $M$ , that we term  $Pr_{\mathcal{B}}(n = j; M, P(d_0, d_1))$ . From the above, we estimate  $\hat{P}(d_0, d_1)$ , the probability parameter maximising the log-likelihood of the observations for every  $(d_0, d_1)$ :

$$\hat{P}(d_0, d_1) = \arg \max_P L(d_0, d_1; M, P), \quad (2)$$

where

$$L(d_0, d_1; M, P) = \sum_{j=1}^M [Pr(n = j|d_0, d_1) \cdot \log Pr_{\mathcal{B}}(n = j; M, P)] \quad (3)$$

is the likelihood of the obtained 2AFC answers having been generated from a binomial distribution with parameters  $P(d_0, d_1)$  and  $M$ . The distribution  $\hat{P}(d_0, d_1)$  that maximises the likelihood of the empirical data originating from the assumed binomial distribution is given by

$$\hat{P}(d_0, d_1) = \frac{1}{M} \sum_{j=1}^M j \cdot Pr(n = j|d_0, d_1), \quad (4)$$

with a derivation in Appendix C. It is important to note that the modelling of the decision-making process does not depend on  $M$ , but contributes to the empirical data and informs us the number of votes per triplets, allowing us to evaluate with a variable number of judgements with the same underlying learned distribution.

Finally, we average the local (in  $(d_0, d_1)$ ) optimal log-likelihood  $\hat{L}(d_0, d_1) = L(d_0, d_1; M, \hat{P}(d_0, d_1))$  on the whole  $(d_0, d_1)$  plane providing a global evaluation of how well the binomial distribution with the  $d$  distance fits the empirical 2AFC data. Fig. 1 shows an example of the method, using a small amount of data points.

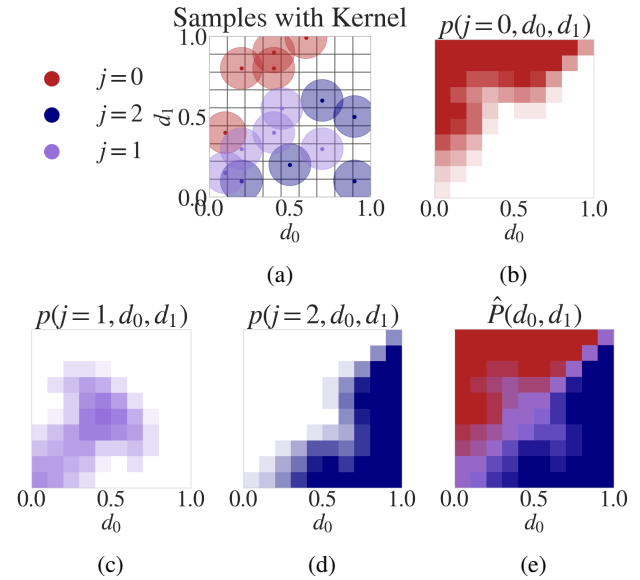


Figure 1: An example using 5 data points,  $M = 2$  for each  $j = \{0, 1, 2\}$ . (a) Samples with a Gaussian kernel applied (the circle represents the standard deviation) and a  $10 \times 10$  grid for which we estimate Eq. 1. (b), (c) and (d) are the estimated conditional distributions for each value of  $j$  with  $M = 2$ , and (e) is the distribution after maximum likelihood estimation according to Eq. 4.

### 3.2. Maximum-likelihood using a neural network

Zhang et al. (2018) use a neural network to minimise the cross-entropy between the output of the network and the proportion  $n(t)/M$ . For comparison to the proposed density estimation method, we use a neural network to estimate  $\hat{P}(d_0, d_1)$  by maximising the likelihood of the training judgements, assuming a binomial distribution. This allows for a more complex function, whilst adhering to the same assumptions of the proposed method.

Given a training set of size  $T$ , where each sample consists of the triplet  $\{d_0(t), d_1(t), n(t)\}$ , as defined in earlier sections, we propose to minimise the negative log-likelihood over the

set of measurements according to a binomial distribution;

$$\begin{aligned} \text{NLL}(\{n(t), t = 1 \dots T\}, \hat{P}, M) = \\ - \frac{1}{T} \sum_{t=0}^T \log \text{Pr}_{\mathcal{B}}(n(t); M, \hat{P}(d_0(t), d_1(t))). \end{aligned} \quad (5)$$

As in the previous section, to implement symmetry, we extend the training dataset with mirrored examples leading to  $2T$  training samples, i.e.,  $\{d_0(t), d_1(t), n(t)\}$  and  $\{d_1(t), d_0(t), M - n(t)\}$ .

### 3.3. Evaluation Metrics

We propose several evaluation metrics to compare the fitting of the binomial to each distance model. Two types of evaluation metrics will be used; (1) based on the agreement of decisions from the model, and (2) based on the log-likelihood of judgements according to the learned binomial distribution.

If we apply the criterion of comparing the most likely outcome of the binomial distribution  $\mathcal{B}(M, P)$ , which is  $\lfloor (M + 1)P \rfloor$  (Feller, 1991), with the actual judgement  $n(t)$ , both normalised to  $M$  for each triplet, we obtain a percentage agreement between our probability model  $\mathcal{B}(M, \hat{P}(d_0(t), d_1(t)))$  and the human judgements  $n(t)$ , yielding the following expression:

$$\begin{aligned} \text{AJ}(\{n(t), t = 1 \dots T\}, \hat{P}, M) = \\ 100 - \frac{100}{T} \sum_{t=1}^T \left| \frac{\lfloor (M + 1)\hat{P}(d_0(t), d_1(t)) \rfloor - n(t)}{M} \right|. \end{aligned} \quad (6)$$

Note that the  $M$  used here corresponds to the judgement  $n(t)$ , using the already fit probability model  $\hat{P}$ . The  $M$  used in the evaluation can be different from the one used in the estimation of  $\hat{P}$ , for example, when a test set contains a different number of judgements. We can also generate samples from our learned model and evaluate the agreement with the training data, details can be found in Appendix D

Due to our assumptions of an underlying probability model for the decision process, we can also evaluate log-likelihoods of judgements according to the estimated binomial parameter. Rather than just measure the percentage of judgements that agree with our model, we can evaluate the negative log-likelihood of the empirical data according to the learned binomial model given by Eq. 5.

Finally, a regularly used metric is the agreement purely between the decisions; *does the perceptual distance select the same distorted image as the humans?* For a set of experi-

ments, this is given by

$$\begin{aligned} 2\text{AFC} = \frac{1}{T} \sum_{t=1}^T \left[ \hat{p}(d_0(t), d_1(t)) \cdot \frac{n(t)}{M} + \right. \\ \left. \left(1 - \frac{n(t)}{M}\right) \cdot \left(1 - \hat{p}(d_0(t), d_1(t))\right) \right], \end{aligned} \quad (7)$$

where  $n(t)$  is the number of humans that selected the first distorted image as closer to the reference, and  $\hat{p} \in \{0, 1\}$  is the preference of the perceptual distance model i.e. if  $d_0 > d_1$ .

### 3.4. Extension to different number of judgements

We can generalise the result from the previous section to a different number of judgements  $M$  per triplet  $t$ ,  $M_t$ , by transforming the  $M_t$  judgements of each given triplet into binary judgements ( $M = 1$ ) on  $M_t$  identical triplets. Now we can construct the conditional distributions  $p(j = \{0, 1\}, d_0, d_1)$ , where the  $P$  that maximises the likelihood of empirical probabilities is simply  $\hat{P}(d_0, d_1) = p(j = 1, d_0, d_1) / p(d_0, d_1)$ . For example, where  $M = 2$  and both participants select  $\mathbf{x}_0$  ( $n(t) = 2$ ), this is equivalent to two individual judgements preferring  $\mathbf{x}_0$  in two identical triplets. The evaluation metrics remain consistent, but using  $M_t$  for each judgement rather than  $M$ .

## 4. Experiments

We can apply our likelihood model to existing perceptual distances, using maximum likelihood to fit a probability model to the pairs of distances  $\{d_0, d_1\}$ . We do so for 6 candidate distances, and use the training set of the BAPPS dataset, containing triplets in the form  $\{\mathbf{x}_{ref}, \mathbf{x}_0, \mathbf{x}_1\}$  which are patches of size  $64 \times 64$ . The training set contains  $M = 2$  judgements, so the possible values of preference  $n(t)/M$  are limited to the set  $\{0.0, 0.5, 1.0\}$ , where 0.0 means that both observers deem  $\mathbf{x}_0$  to be closer to the reference image than  $\mathbf{x}_1$ . We evaluate our models on the BAPPS validation set, which contains  $M = 5$  judgements. Note that, given we are directly estimating  $P(d_0, d_1)$ , we can train and evaluate on a different number of  $M$  judgements. To obtain a smooth PDF from the set of discrete  $\{d_0, d_1\}$  samples, we use a Gaussian kernel with a constant width, where after uniformisation, the range of  $\{d_0, d_1\}$  is  $[0, 1]$ . The width  $\sigma$  can be set by the user – in our experiments, we found that the method was robust to different  $\sigma$  values, but depended on the amount of data that covers the plane, i.e., less data requires a larger  $\sigma$ . For the BAPPS dataset, we set  $\sigma = \frac{1}{44}$ . We use a  $20 \times 20$  grid to estimate the conditionals in Eq. 1. Sec. 5 examines the proposed method’s robustness to changes in these hyperparameters. Code will be released upon acceptance.

For our comparison, we use the neural network architec-

ture from Zhang et al. (2018) to estimate  $\hat{P}(d_0, d_1)$ . The architecture is two fully connected layers, with 32 channels, followed by a 1 channel fully connected layer with sigmoid activation to ensure the output is in  $[0, 1]$ . We train the model for 5 epochs, batch size of 128 and Adam optimiser with a learning rate of 0.001. Note that for each epoch, each data point is seen twice as we try to implement (but not strictly enforce) symmetry in  $\hat{P}$  by using  $\{d_0(t), d_1(t), n(t)\}$  and  $\{d_1(t), d_0(t), M - n(t)\}$ .

## 5. Results

We evaluate the metrics in Sec. 3.3 for the test set of BAPPS. Table 1 contains the results after optimising separate binomial models for each of our six distance models. The first three models (Euclidean, NLPD and SSIM) achieve similar results in agreement measures and negative log-likelihoods. The three deep-learning-based models (PIM, LPIPS and DISTs) achieve superior performance. Evaluation metrics on simulated judgements from the learned models and the training set can be seen in Appendix E. Table 2 compares the 2AFC score using just the raw distance, vs using  $\hat{P}(d_0, d_1)$  (as in Table 1). Most distances see just a slight increase in score, apart from Euclidean and LPIPS. Note that LPIPS parameters have been optimised to explicitly minimise the cross-entropy the network outputs and the ground truth proportion  $n(t)/M$ .

As our density estimation method is deterministic, the standard deviation of the evaluation metrics in Table 1 is 0.0. However, with neural networks, there is a slight deviation between runs due to the stochastic nature of training, with a standard deviation of the 2AFC score above 1.0 for all metrics except DISTs. This also caused us to exclude one of the runs using PIM, as training became unstable.

In addition, we can visualise  $\hat{P}(d_0, d_1)$  for different distances, to see the separation or amount of uncertainty along the diagonal, where  $d_0$  and  $d_1$  are similar. Fig. 2 shows  $\hat{P}(d_0, d_1)$ , revealing that the three deep-learning-based metrics offer more certainty in the top left ( $d_0 \ll d_1$ ) and bottom right ( $d_0 \gg d_1$ ). As the distances  $\{d_0, d_1\}$  increase (top right), the uncertainty region grows smaller, reflecting how humans perceive sharper differences in images far from the reference. The traditional distances display a wider area around  $0.3 < \hat{P}(d_0, d_1) < 0.7$ , indicating higher uncertainty on the decision. In comparison, the neural networks display non-symmetric unpredictable behaviour in Euclidean, NLPD and SSIM, as symmetry is not strictly enforced, and overconfidence in judgements when using PIM, LPIPS and DISTs.

Additionally, we compare training time and number of parameters between the proposed density estimation method and that using neural networks. The parameters in density

estimation are the grid for which we estimate  $\hat{P}(d_0, d_1)$  for, where we use a  $20 \times 20$  grid resulting in 400 parameters, compared to 1281 in the neural network. Density estimation is also significantly faster to train. Over 10 training runs, the minimum training time (giving a quickest time possible) for density estimation was 4.5s and for neural networks 43.3s, despite neural networks utilising a GPU. More details can be found in Appendix G.

**Interpretability** One advantage of explicitly modelling the decision is that we can evaluate the negative log-likelihood of different  $n(t)$  values using Eq. 5, allowing users to query the model for a given perceptual distance model. This holds for both the proposed density estimation and the neural network when optimised for log-likelihood. Fig 3 shows the negative log-likelihood of a different number of observers  $j = [0, 5]$  preferring the far right image over the middle, according to the density estimation method. (See other examples Appendix F). Practitioners can see where a certain perceptual distance model fails, assess the probability of the decision, and how the likelihood will change with changes in  $(d_0, d_1)$  and the number of judgements  $M$ .

**Robustness** There are two hyperparameters of interest in the proposed method; the width of the Gaussian window  $\sigma$  for smoothing, and the resolution of the grid used to estimate  $\hat{P}(d_0, d_1)$ . We find the optimal  $\hat{P}(d_0, d_1)$  for the training set of BAPPS ( $M = 2$ ) by continuously varying the chosen hyperparameter, and plot the negative log-likelihood and percentage agreement when evaluating on the test set ( $M = 5$ ).

The kernel width sets the amount of smoothing applied to our point-wise estimates from the training set. We test a range of values  $\sigma \in [0.0037, 1]$ , and fix the grid to  $100 \times 100$  such that the grid is not the limiting factor. Fig. 4a shows that a large  $\sigma$  (heavy smoothing) results in performance loss, with a large flat section for  $\sigma < 0.1$  that achieves similar performance. The ability to visualise the decision surface (Fig 2) allows the user to decide a  $\sigma$  that determines the smoothness of the estimated distribution  $\hat{P}(d_0, d_1)$ . A clear advantage over neural networks is that the kernel width and grid have clear and predictable effects on the resulting model, compared to adjusting the hyperparameters of a network or optimiser used, and allows users to control aspects of the model in a clear and easy manner.

The grid size sets the resolution of  $\hat{P}(d_0, d_1)$ . Fig. 1 (a) shows an example of a  $10 \times 10$  grid on data in  $[0, 1]$ . We test grid sizes in the range  $[5, 100]$ . Fig. 4b shows that a too coarse grid does not allow proper estimation, and more partitions than roughly 20 see no gain in performance. The lower the grid size, the less parameters and the less computation needed to construct the estimation. This also depends on the spread of data in  $\{d_0, d_1\}$  after marginal uniformisation, but

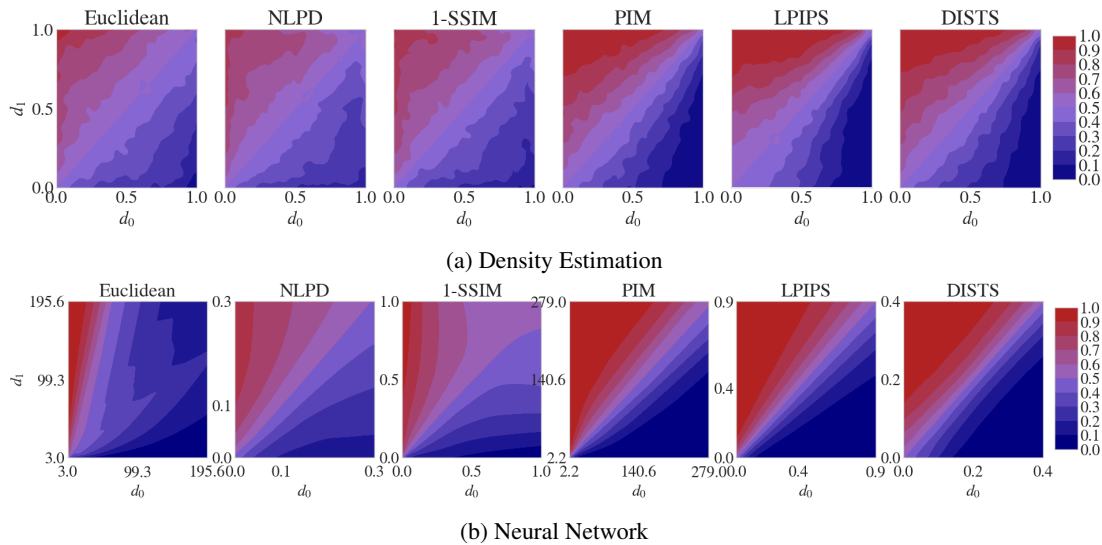


Figure 2: Binomial parameter  $P$  estimated from the BAPPS training set for different perceptual distance models using (a) Density estimation and (b) Neural network.

Table 1: Evaluation metrics on the BAPPS validation set ( $M = 5$ ). Reported is the mean and standard deviation over 10 runs. Lower NLL is better. Note that for PIM, we had to disregard one of the runs as the training became unstable.

	Measure	Euclidean	NLPD	SSIM	PIM	LPIPS	DISTS
Density Estimation	AJ( $n, \hat{P}, M$ ) % $\uparrow$	75.89 $\pm$ 0.00	75.82 $\pm$ 0.00	76.17 $\pm$ 0.00	82.12 $\pm$ 0.00	82.43 $\pm$ 0.00	81.34 $\pm$ 0.00
	NLL( $n, \hat{P}, M$ ) $\downarrow$	1.86 $\pm$ 0.00	1.86 $\pm$ 0.00	1.84 $\pm$ 0.00	1.49 $\pm$ 0.00	1.46 $\pm$ 0.00	1.53 $\pm$ 0.00
	2AFC Score % $\uparrow$	63.46 $\pm$ 0.00	63.31 $\pm$ 0.00	63.65 $\pm$ 0.00	70.09 $\pm$ 0.00	68.94 $\pm$ 0.00	69.12 $\pm$ 0.00
Neural Network	AJ( $n, \hat{P}, M$ ) % $\uparrow$	75.76 $\pm$ 0.09	75.79 $\pm$ 0.08	76.18 $\pm$ 0.18	82.07 $\pm$ 0.13	82.55 $\pm$ 0.03	81.40 $\pm$ 0.03
	NLL( $n, \hat{P}, M$ ) $\downarrow$	1.87 $\pm$ 0.00	1.86 $\pm$ 0.00	1.84 $\pm$ 0.01	1.50 $\pm$ 0.01	1.46 $\pm$ 0.00	1.53 $\pm$ 0.00
	2AFC Score % $\uparrow$	62.43 $\pm$ 1.31	63.78 $\pm$ 1.20	64.19 $\pm$ 1.37	70.31 $\pm$ 1.34	70.02 $\pm$ 1.04	68.81 $\pm$ 0.49

for data similarly distributed to BAPPS, one would expect a stable performance across grid sizes. The behaviour of both the kernel width and grid size is also consistent across distances.

### 5.1. Different number of judgements

We also present results on the Challenge on Learned Image Compression (CLIC) 2021 dataset, which contains  $t$  triplets with different numbers of judgements  $M_t$ . Judgements which used an ‘‘anchor’’, where one of the distorted images is the reference image, are removed as including these images interacts with the uniformisation transform as they are on the edge of the support ( $d_0$  or  $d_1 = 0.0$ ). We use the oracle set to optimise, and the validation set to evaluate. The oracle set contains 119,901 triplets with  $M_t = \{1, 2\}$  and the validation set contains 4807 triplets with  $M_t \in [1, 10]$ , although a large percentage have one judgement. The distribution of  $M_t$  can be seen in Appendix H. We train the neural networks using the same hyperparameters in the previous section.

With CLIC, Euclidean, NLPD, and SSIM struggle to dis-

tinguish between distorted images, as seen in Table 3. This is due to the non-uniformity in the CLIC measurements, despite the marginal uniformisation, seen in Appendix H, where these three distances display a large amount of uncertainty in the surface. More data could alleviate this issue, for a smooth and consistent estimation of  $\hat{P}(d_0, d_1)$ . PIM, LPIPS, and DISTs display much more expected behaviour, with PIM achieving a 2AFC score on the test set of 0.7305. We observe similar behaviour in the neural network models, with higher variation between runs for Euclidean and NLPD.

## 6. Conclusions

We present a method for evaluating the ability of perceptual distance models to explain two-alternative forced choice experimental data, using a simple assumption about the observer’s decision-making process. We rely on kernel smoothing and marginal uniformisation to compute a smooth and consistent estimate of the involved PDFs on the 2-distance plane  $(d_0, d_1)$ , where maximum likelihood is applied to estimate the choice weight given a pair of distance values from

Table 2: 2AFC Scores (Eq. 7) on the BAPPS test set, where distance only is checking if  $d_0 > d_1$ , and  $\hat{P}(d_0, d_1)$  is our approach. \*LPIPS has been optimised to replicate decisions in the BAPPS training set using a neural network mapping  $(d_0, d_1)$  to  $n(t)/M$ .

2AFC Score % $\uparrow$	Euclidean	NLPD	SSIM	PIM	LPIPS*	DISTS
Distance Only	63.38 $\pm$ 0.00	62.71 $\pm$ 0.00	63.11 $\pm$ 0.00	69.26 $\pm$ 0.00	69.40 $\pm$ 0.00	68.48 $\pm$ 0.00
Density Estimation	63.46 $\pm$ 0.00	63.31 $\pm$ 0.00	63.65 $\pm$ 0.00	70.09 $\pm$ 0.00	68.94 $\pm$ 0.00	69.12 $\pm$ 0.00
Neural network	62.43 $\pm$ 1.31	63.78 $\pm$ 1.20	64.19 $\pm$ 1.37	70.31 $\pm$ 1.34	70.02 $\pm$ 1.04	68.81 $\pm$ 0.49

Table 3: Results on the CLIC validation set ( $M_t = [1, 10]$ ). Reported is the mean and standard deviation over 10 runs. Lower NLL is better

	Measure	Euclidean	NLPD	SSIM	PIM	LPIPS	DISTS
Density Estimation	AJ( $n, \hat{P}, M$ ) % $\uparrow$	44.27 $\pm$ 0.00	44.70 $\pm$ 0.00	44.85 $\pm$ 0.00	74.02 $\pm$ 0.00	74.03 $\pm$ 0.00	75.99 $\pm$ 0.00
	NLL( $n, \hat{P}, M$ ) $\downarrow$	0.72 $\pm$ 0.00	0.72 $\pm$ 0.00	0.73 $\pm$ 0.00	0.62 $\pm$ 0.00	0.61 $\pm$ 0.00	0.58 $\pm$ 0.00
	2AFC Score % $\uparrow$	42.94 $\pm$ 0.00	43.08 $\pm$ 0.00	43.62 $\pm$ 0.00	73.18 $\pm$ 0.00	73.14 $\pm$ 0.00	75.39 $\pm$ 0.00
Neural Network	AJ( $n, \hat{P}, M$ ) % $\uparrow$	46.25 $\pm$ 1.04	45.86 $\pm$ 3.01	45.13 $\pm$ 0.18	73.89 $\pm$ 0.08	73.97 $\pm$ 0.06	75.87 $\pm$ 0.05
	NLL( $n, \hat{P}, M$ ) $\downarrow$	0.73 $\pm$ 0.00	0.72 $\pm$ 0.00	0.76 $\pm$ 0.00	0.62 $\pm$ 0.01	0.61 $\pm$ 0.00	0.58 $\pm$ 0.00
	2AFC Score % $\uparrow$	45.01 $\pm$ 1.09	44.45 $\pm$ 3.05	43.85 $\pm$ 0.18	73.20 $\pm$ 0.09	73.14 $\pm$ 0.06	75.26 $\pm$ 0.04

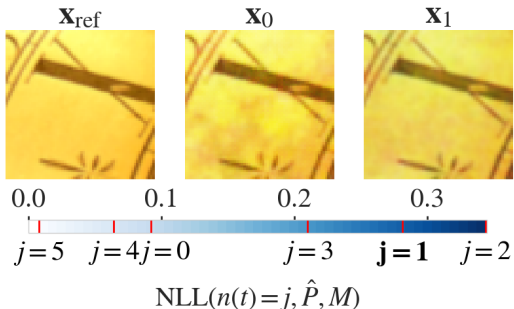


Figure 3: An example of evaluating the density estimation probability model for different  $j = [0, 5]$ , for a triplet from the BAPPS test set, according to DISTS where the true  $j$  is shown in bold. Shown above the colour bar is negative log-likelihood, where white is more likely and blue is less.

the perceptual model. We apply it to the BAPPS dataset, obtaining a similar ranking for the visual models as in previous works but with additional insights from the richer pool of evaluation metrics. The method is robust to changes in the values of its two hyperparameters, allowing practitioners to quickly and reliably evaluate perceptual distance models without requiring additional training or tuning. We achieve similar performance to a neural network optimised to maximise the likelihood of judgements, with an order of magnitude less parameters and training time, and interpretable hyperparameters.

Traditional perceptual datasets use a ranking algorithm to decide which triplets to show the observer. Our method does not utilise this information, as it assumes the triplets are randomly selected. As ranking is expensive in terms of the required number of judgements and does not scale

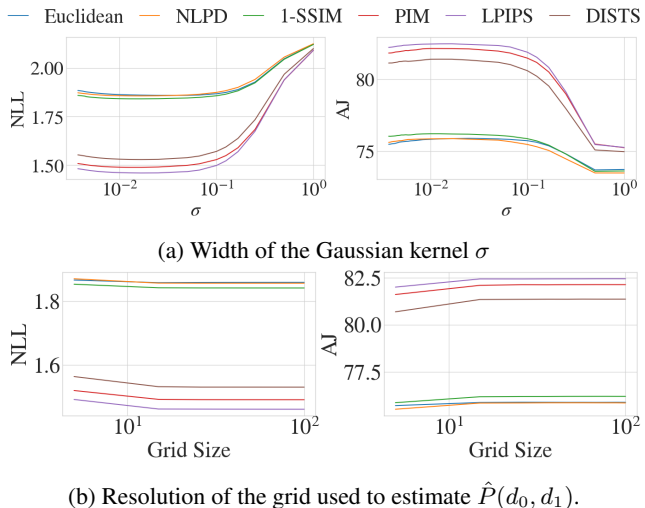


Figure 4: Robustness of the density estimation method with relation to (a) the width of the Gaussian kernel  $\sigma$  and (b) the grid used to estimate  $\hat{P}(d_0, d_1)$ . In each subplot, left is NLL (Eq. 4), right is AJ (Eq. 6).

well to large amounts of data, the number of triplets tends to be low. In contrast, our method requires a large number of samples to ensure reliable PDF estimations, which is consistent with more recent crowd-sourced datasets. Regarding possible extensions, a distance model can be optimised for maximising the log-likelihood according to the density estimation method. This could lead to metrics like LPIPS, where the distance model is optimised based on the judgement data. Another line is to analyse the practical impact of the mismatch between the numbers of judgements  $M$  in training and testing. Note that, although  $\hat{P}(d_0, d_1)$  does not depend on  $M$ , the data used to estimate the PDF does.



## Impact Statement

This paper presents work whose goal is to advance the field of computer vision. Outside of existing ethical issues for this area, such as bias in existing datasets, there are no issues which we feel must be specifically highlighted here.

## References

- Bhardwaj, S., Fischer, I., Ballé, J., and Chinen, T. An unsupervised information-theoretic perceptual quality metric. *Advances in Neural Information Processing Systems*, 33: 13–24, 2020.
- Ding, K., Ma, K., Wang, S., and Simoncelli, E. P. Image quality assessment: Unifying structure and texture similarity. *arXiv preprint arXiv:2004.07728*, 2020.
- Fechner, G. T. Elements of psychophysics, 1860. 1948.
- Feller, W. *An introduction to probability theory and its applications, Volume 2*, volume 81. John Wiley & Sons, 1991.
- Hepburn, A., Laparra, V., Malo, J., McConville, R., and Santos-Rodríguez, R. Perceptnet: A human visual system inspired neural network for estimating perceptual distance. In *IEEE ICIP 2020*, pp. 121–125. IEEE, 2020.
- Jogan, M. and Stocker, A. A. A new two-alternative forced choice method for the unbiased characterization of perceptual bias and discriminability. *Journal of Vision*, 14(3):20–20, 2014.
- Kingdom, F. A. A. and Prins, N. *Psychophysics: A practical introduction*. Elsevier Academic Press, 2010.
- Laparra, V., Camps-Valls, G., and Malo, J. Iterative gaussianization: from ica to random rotations. *IEEE transactions on neural networks*, 22(4):537–549, 2011.
- Laparra, V., Ballé, J., Berardino, A., and P, S. E. Perceptual image quality assessment using a normalized laplacian pyramid. *Electronic Imaging*, 2016(16):1–6, 2016.
- Larson, E. C. and Chandler, D. M. Most apparent distortion: full-reference image quality assessment and the role of strategy. *JEI*, 19(1):011006, 2010.
- Maloney, L. T. and Yang, J. N. Maximum likelihood difference scaling. *Journal of Vision*, 3(8):5–5, 2003.
- Ponomarenko, N. et al. Tid2008-a database for evaluation of full-reference visual quality assessment metrics. *Advances of Modern Radioelectronics*, 10(4):30–45, 2009.
- Ponomarenko, N. et al. Color image database tid2013: Peculiarities and preliminary results. In *EUVIP*, pp. 106–111. IEEE, 2013.
- Sheikh, H. R., Wang, Z., Cormack, L., and Bovik, A. C. Live image quality assessment database release 2. <http://live.ece.utexas.edu/research/quality>, 2005.
- Silverstein, D. A. and Farrell, J. E. Efficient method for paired comparison. *Journal of Electronic Imaging*, 10(2): 394–398, 2001.
- Thurstone, L. L. A law of comparative judgment. *Psychological review*, 101(2):266, 1994.
- Toderici, G., Theis, L., Ballé, J., Johnston, N., Shi, W., Agustsson, E., Rapaka, K., Mentzer, F., Sinno, Z., Norkin, A., Noury, E., and Timofte, R. Workshop and challenge on learned image compression (clic2021), 2021. URL <http://www.compression.cc>.
- Tsukida, K., Gupta, M. R., et al. How to analyze paired comparison data. *Department of Electrical Engineering University of Washington, Tech. Rep. UWEETR-2011-0004*, 1, 2011.
- Wang, Z., Simoncelli, E. P., and Bovik, A. C. Multiscale structural similarity for image quality assessment. In *ACSSC*, volume 2, pp. 1398–1402. Ieee, 2003.
- Wang, Z., Bovik, A., Sheikh, H., and Simoncelli, E. Image quality assessment: from error visibility to structural similarity. *IEEE Transactions on Image Processing*, 13(4):600–612, 2004. doi: 10.1109/TIP.2003.819861.
- Zhang, R., Isola, P., Efros, A., Shechtman, E., and Wang, O. The unreasonable effectiveness of deep features as a perceptual metric. In *Proceedings of the IEEE CVPR*, pp. 586–595, 2018.

## A. Perceptual Datasets

Table 4 shows the existing perceptual datasets, and what sort of experimental setup was used. Whilst most datasets use the 2AFC setup, some datasets (TID, CSIQ, CLIC) use an Elo ranking system to decide which images to show a particular observer. This results in a dataset where each triplet judgement is not independent, and results in triplets having a different number of judgements  $M$ .

BAPPS and CLIC are the only datasets that release the raw 2AFC ratings, but they differ in that BAPPS ensures the same number of judgements for each triplet, and each observer is shown random triplets. This is the setting that the proposed method was designed for, but we can still apply it to others.

Table 4: Detailed description of existing perceptual datasets: TID 2008(Ponomarenko et al., 2009), TID 2013(Ponomarenko et al., 2013), CSIQ (Larson & Chandler, 2010), LIVE (Sheikh et al., 2005), BAPPS (Zhang et al., 2018) and CLIC (Toderici et al., 2021).

Dataset	Method	Image Sizes	No. of Images	No. of Distortions	No. of Triplets	Total No. of Judgements	Type of Judgement Released
TID 2008	2AFC sorting	512x384	25	17	2k	256k	MOS
TID 2013	2AFC sorting	512x384	25	24	3k	5k	MOS
CSIQ	2AFC	512x512	30	6	866	5k	DMOS
LIVE	5 level scale	768x512	29	5	779	25k	DMOS
BAPPS Train	2AFC	64x64	151k	425	151k	302k	2AFC
BAPPS JND	JND	64x64	10k	425	10k	29k	True/False
BAPPS Validation	2AFC	64x64	36k	425+	36k	182k	2AFC
CLIC 2021	2AFC	768x768	315		119k	120k	2AFC

## B. Marginal Uniformisation

The most common approach to estimate a smooth function from a set of discrete events is to use adaptive kernels, with sizes depending on the density of values at a given point when estimating the density. Alternatively, we can search for transformations relocating the samples such that they cover the space fully and as evenly as possible. In this work, for each candidate distance, we transform the pairs of distances  $\{d_0, d_1\}$ , such that the resulting set of points is marginally uniform in the range  $[0, 1]$ . The marginal uniformisation transform is given by the histogram-equalisation solution

$$u = U_{(k)}^i(x_i^{(k)}) = \int_{-\infty}^{x_i^{(k)}} p_i(x_i'^{(k)}) dx_i'^{(k)}. \quad (8)$$

where  $x_i^{(k)}$  is a sample in the  $k$ th marginal and  $p_i$  is approximated with histograms, for which computing the cumulative density function is straightforward (Laparra et al., 2011). In doing so we are transforming our data to a (fairly) uniform domain. This non-linear transformation facilitates the numerical density estimations from the discrete data but it is transparent for the posterior computations. Fig.5 shows some examples of distances transformed to a uniform domain.

## C. Maximum likelihood density estimation

We have that:

$$Pr_{\mathcal{B}}(n = j; M, P) = \frac{M!}{j!(M-j)!} P^j (1-P)^{M-j}, \quad (9)$$

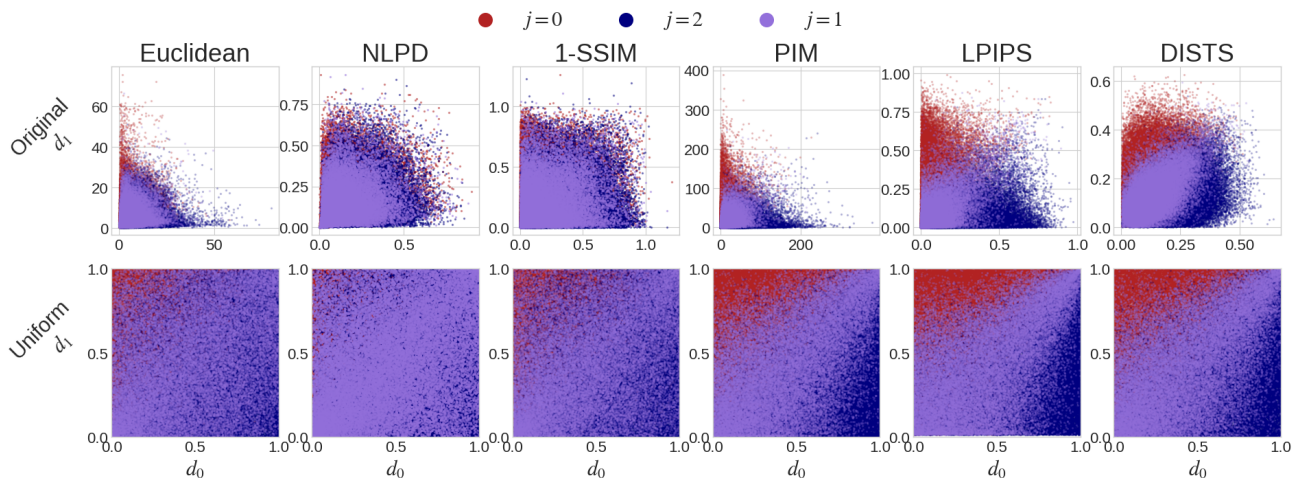


Figure 5: Scatter plot of candidate distances in their original space (top row) and uniformised (bottom row). Shown are the training samples from the BAPPS dataset and the colour indicates the judgement assigned to triplet according to 2 observers.

We use the latter expression in Eq. 3 for choosing the  $P$  that maximises the likelihood of the empirical probabilities  $\{Pr(n = j|d_0, d_1)\}$ :

$$\begin{aligned} \hat{P}(d_0, d_1) &= \arg \max_P \sum_{j=1}^M Pr(n = j|d_0, d_1) \left[ \log \left( \frac{M!}{j!(M-j)!} \right) + j \log P \right. \\ &\quad \left. + (M-j) \log(1-P) \right] \\ &= \frac{1}{M} \sum_{j=1}^M j \cdot Pr(n = j|d_0, d_1), \end{aligned} \quad (10)$$

where the last equality is obtained by differentiating the argument of the right-hand side in the first equation w.r.t.  $P$ , equating to 0 and solving for  $P$ .

## D. Additional Evaluation

To maximise the agreement for the learned model, one can generate random samples  $\hat{n}(t)$  from our learned distribution  $\hat{n}(t) \sim \mathcal{B}(M, \hat{P}(d_0(t), d_1(t)))$ , and see the agreement between the empirical and the simulated judgements, according to our learned model. This provides a reference for the case that the observed judgements follow the fitted binomial model exactly.

Similarly to the agreement of judgements, we can sample from our learned distribution with  $M$  judgements  $\hat{n}(t) \sim \mathcal{B}(M, \hat{P}(d_0(t), d_1(t)))$  and evaluate the negative log-likelihoods of these judgements, to get a minimum possible negative log-likelihood achieved by a distance.

Both of these measures are reported for samples generated from the learned models, evaluated against the training data, with  $AJ(\hat{n}, \hat{P}, M)$  and  $NLL(\hat{n}, \hat{P}, M)$ .

## E. BAPPS Additional Results

Here we present additional results on the training and test validation sets of BAPPS. We also separately report evaluation metrics per distortion used in the BAPPS test set for a more in-depth comparison of metrics.

Table 5 shows evaluation metrics on both the training and test set of BAPPS using the proposed density estimation method. The training set has been used to fit  $\hat{P}(d_0, d_1)$ . We see a consistent behaviour across sets, despite the different number of judgements  $M$  for the train and test sets. Table 6 reports the same measurements for the neural network method, displaying similar behaviour.

Table 5: Results on the BAPPS dataset (Zhang et al., 2018) using the density estimation method. Since this method is deterministic, we report only the value. In the training set, there are 2 judgements per triplet ( $M = 2$ ) and in the test set, 5 ( $M = 5$ ). Lower NLL is better.  $\hat{n}$  denotes sampling judgements from the model optimised using the training data and evaluating against the true judgements.

Measure		Euclidean	NLPD	SSIM	PIM	LPIPS	DISTS
$AJ(n, \hat{P}, M) (\%) \uparrow$	Train	69.38	69.16	71.29	80.52	80.60	79.65
	Test	75.89	75.82	76.17	82.12	82.43	81.34
$AJ(\hat{n}, \hat{P}, M) (\%) \uparrow$	Train	74.90	74.26	75.40	81.85	82.20	81.23
	Test	83.02	83.05	83.25	84.98	85.37	84.86
$NLL(n, \hat{P}, M) \downarrow$	Train	1.05	1.07	1.02	0.76	0.75	0.78
	Test	1.86	1.86	1.84	1.49	1.46	1.53
$NLL(\hat{n}, \hat{P}, M) \downarrow$	Train	0.93	0.94	0.91	0.72	0.71	0.74
	Test	1.47	1.47	1.45	1.31	1.29	1.33
2AFC Score $\uparrow$	Train	66.80	66.50	68.88	77.69	77.05	76.61
	Test	62.43	63.78	64.19	70.31	70.02	68.81

Table 6: Results on the BAPPS dataset (Zhang et al., 2018) using a neural network. In the training set, there are 2 judgements per triplet ( $M = 2$ ) and in the test set, 5 ( $M = 5$ ). Lower NLL is better.  $\hat{n}$  denotes sampling judgements from the model optimised using the training data and evaluating against the true judgements.

Measure		Euclidean	NLPD	SSIM	PIM	LPIPS	DISTS
$AJ(n, \hat{P}, M) (\%) \uparrow$	Train	69.28 $\pm$ 0.12	69.05 $\pm$ 0.12	71.20 $\pm$ 0.16	80.48 $\pm$ 0.02	80.59 $\pm$ 0.01	79.65 $\pm$ 0.01
	Test	75.76 $\pm$ 0.09	75.79 $\pm$ 0.08	76.18 $\pm$ 0.18	82.07 $\pm$ 0.13	82.55 $\pm$ 0.03	81.40 $\pm$ 0.03
$AJ(\hat{n}, \hat{P}, M) (\%) \uparrow$	Train	74.96 $\pm$ 0.30	74.18 $\pm$ 0.21	75.54 $\pm$ 0.55	81.83 $\pm$ 0.77	82.51 $\pm$ 0.17	81.55 $\pm$ 0.23
	Test	83.11 $\pm$ 0.11	82.95 $\pm$ 0.06	83.19 $\pm$ 0.13	85.05 $\pm$ 0.36	85.43 $\pm$ 0.07	85.00 $\pm$ 0.11
$NLL(n, \hat{P}, M) \downarrow$	Train	1.05 $\pm$ 0.00	1.07 $\pm$ 0.00	1.02 $\pm$ 0.00	0.76 $\pm$ 0.00	0.75 $\pm$ 0.00	0.78 $\pm$ 0.00
	Test	1.87 $\pm$ 0.00	1.86 $\pm$ 0.00	1.84 $\pm$ 0.01	1.50 $\pm$ 0.01	1.46 $\pm$ 0.00	1.53 $\pm$ 0.00
$NLL(\hat{n}, \hat{P}, M) \downarrow$	Train	0.93 $\pm$ 0.01	0.94 $\pm$ 0.01	0.90 $\pm$ 0.01	0.72 $\pm$ 0.03	0.70 $\pm$ 0.01	0.73 $\pm$ 0.01
	Test	1.46 $\pm$ 0.01	1.47 $\pm$ 0.00	1.45 $\pm$ 0.01	1.31 $\pm$ 0.03	1.28 $\pm$ 0.00	1.32 $\pm$ 0.01
2AFC Score $\uparrow$	Train	66.69 $\pm$ 0.06	66.52 $\pm$ 0.06	68.90 $\pm$ 0.10	69.94 $\pm$ 23.31	77.09 $\pm$ 0.05	76.61 $\pm$ 0.03
	Test	62.43 $\pm$ 1.31	63.78 $\pm$ 1.20	64.19 $\pm$ 1.37	63.28 $\pm$ 21.13	70.02 $\pm$ 1.04	68.81 $\pm$ 0.49

Table 7 shows a breakdown of the agreement of judgements (AJ) Eq. 6, negative log-likelihood (NLL) Eq. 5 and 2AFC score Eq. 7, evaluated on the test set of BAPPS. We split the dataset into the category of distortion used, namely: Traditional (4720 triplets), CNN (4720 triplets), Color (9440 triplets), Deblur (1888 triplets), Frame interpolation (10856) and Super resolution (4720 triplets). Details on these distortions can be found in (Zhang et al., 2018).

## F. Interpretability - More Examples

The negative log-likelihood in Eq 5 depends on  $\hat{P}(d_0, d_1)$ , and in order to visualise this, here we present several examples of evaluating the NLL of different  $j = [0, 5]$ . We use triplets where one distorted image is extremely close to the reference and the decision is clear (Fig 6), one distorted image is extremely far from the original and the decision is clear (Fig 7) and finally a triplet where the decision is borderline as both distorted images are far from the original (Fig 8). For all experiments we use the density estimation method for estimation  $\hat{P}(d_0, d_1)$

## G. Method Comparison

Table 8 shows a comparison of the minimum training time, number of parameters, inference time of 1 sample (1 ( $d_0, d_1$ ) pair, and 128 samples. We report minimum training time as this gives a lower bound on how fast the method can train, accounting for other processes happening on the device. The density estimation method was ran on a Intel Xeon W-2245 CPU with 8 cores (16 with hyperthreading) and the neural network was trained on an NVIDIA RTX A5000 gpu.

Table 7: Evaluation metrics on the BAPPS validation set, split by distortion applied for the proposed density estimation method. Since the density estimation method is deterministic, we only report the value.

Distance	Measure	Distortion					
		Traditional	CNN	Color	Deblur	Frame Interp.	Super Resolution
Euclidean	AJ( $n, \hat{P}, M$ ) (%) $\uparrow$	65.54	77.67	78.33	78.31	75.93	76.44
	NLL( $n, \hat{P}, M$ ) $\downarrow$	2.52	1.72	1.73	1.71	1.83	1.82
	2AFC Score $\uparrow$	55.51	80.72	62.10	57.81	56.25	66.18
NLPD	AJ( $n, \hat{P}, M$ ) (%) $\uparrow$	66.44	76.78	76.02	78.32	76.22	77.15
	NLL( $n, \hat{P}, M$ ) $\downarrow$	2.48	1.76	1.84	1.70	1.81	1.78
	2AFC Score $\uparrow$	56.61	80.13	59.24	57.48	55.72	67.07
SSIM	AJ( $n, \hat{P}, M$ ) (%) $\uparrow$	67.86	78.85	76.05	78.43	77.38	76.48
	NLL( $n, \hat{P}, M$ ) $\downarrow$	2.41	1.64	1.85	1.70	1.75	1.82
	2AFC Score $\uparrow$	59.79	80.83	60.13	58.49	57.10	65.01
PIM	AJ( $n, \hat{P}, M$ ) (%) $\uparrow$	81.44	86.99	80.25	81.43	82.02	81.74
	NLL( $n, \hat{P}, M$ ) $\downarrow$	1.54	1.15	1.62	1.55	1.49	1.51
	2AFC Score $\uparrow$	76.69	83.75	65.19	62.15	63.08	71.53
LPIPS	AJ( $n, \hat{P}, M$ ) (%) $\uparrow$	80.58	88.12	80.90	81.03	81.62	82.80
	NLL( $n, \hat{P}, M$ ) $\downarrow$	1.60	1.06	1.56	1.56	1.52	1.44
	2AFC Score $\uparrow$	74.83	83.64	65.49	61.39	58.58	69.84
DISTS	AJ( $n, \hat{P}, M$ ) (%) $\uparrow$	80.33	85.92	79.20	80.17	81.27	81.77
	NLL( $n, \hat{P}, M$ ) $\downarrow$	1.61	1.20	1.66	1.61	1.54	1.51
	2AFC Score $\uparrow$	75.47	83.24	63.96	60.20	62.55	71.36

Table 8: Comparison of minimum training time over 10 runs (giving a lower bound for training time) and number of learnable parameters for the proposed density estimation method and neural network counterpart. The density estimation method was ran on a Intel Xeon W-2245 CPU with 8 cores (16 with hyperthreading) and the neural network was trained on an NVIDIA RTX A5000 gpu.

Method	Minimum Training time (s)	No. of Parameters	Minimum Inference Time 1 sample (s)	Minimum Inference Time 128 samples (s)
Density Estimation	4.5	400	$9.9 \times 10^{-8}$	$3.7 \times 10^{-7}$
Neural Network	43.3	1281	$1.0 \times 10^{-7}$	$4.0 \times 10^{-7}$

## H. CLIC

We include additional information regarding the CLIC dataset used, including the distribution of the number of judgements  $M_t$  per triplet. We also show additional visualisations of the triplets in the  $(d_0, d_1)$  before and after the uniformistaion transformation, as well as evaluation metrics using both the training and test set.

### H.1. Distribution of Number of Judgements

The CLIC 2021 subset we use to train (the oracle set) consists of 119,901 triplets with the number of judgements  $M_t = \{1, 2\}$  and results of the judgements  $j$ , where the distribution can be seen in Fig. 10. We also show the distribution of  $j$  for each  $M_t$ . Most of the triplets have one judgement, with roughly uniform  $j = \{0, 1\}$ . For the triplets with 2 judgements, the majority are indecisive with  $j = 1$ .

The same distribution for the subset used for evaluation (the validation set) with  $M_t = [1, 10]$  can be seen in Fig 9. The vast majority of triplets also contain only 1 judgement, where the distribution of  $j$  similar to that of the training set. The set also includes a small number of triplets with more judgements, varying in distribution of  $j$ .

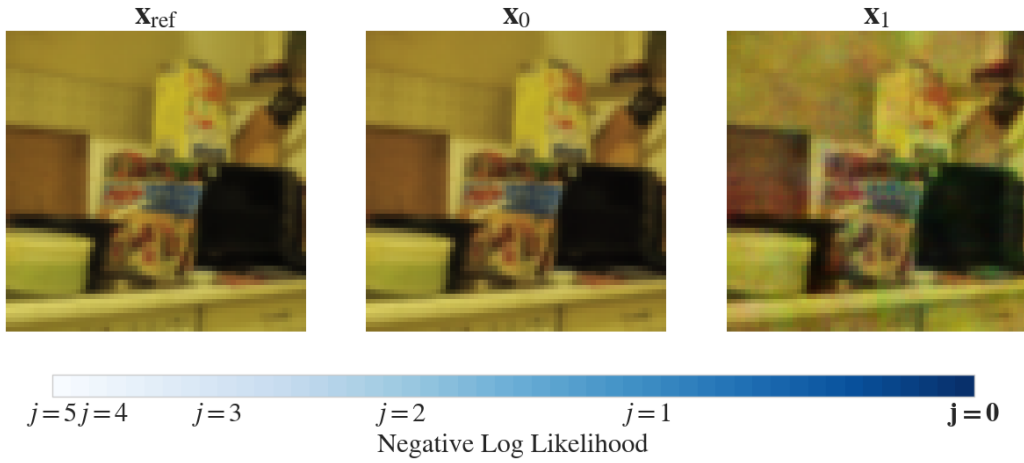


Figure 6: Example of valuating the negative log-likelihood  $j = [0, 5]$  according to DISTS for a triplet from the BAPPS test set where one image  $x_0$  is close to the reference  $x_{\text{ref}}$ . White is more likely and blue is less likely.

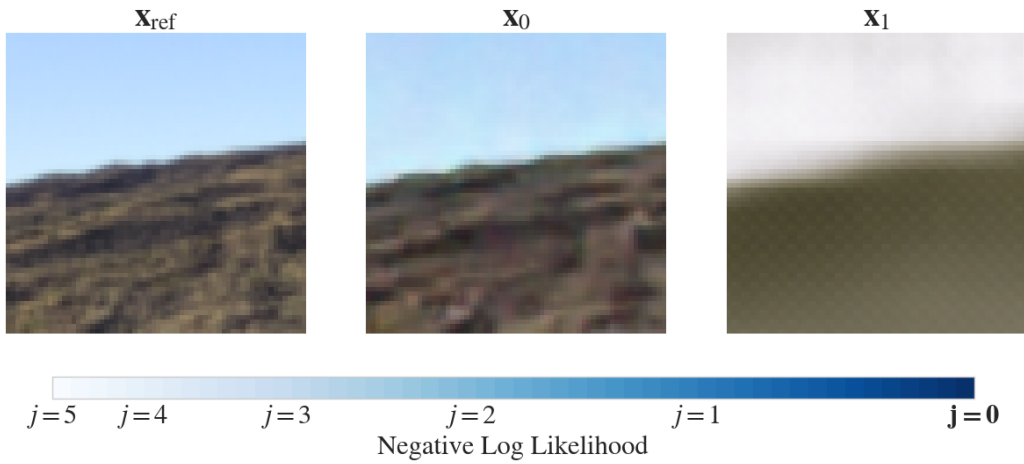


Figure 7: Example of valuating the negative log-likelihood  $j = [0, 5]$  according to DISTS for a triplet from the BAPPS test set where one image  $x_0$  is far from the reference  $x_{\text{ref}}$ . White is more likely and blue is less likely.

## H.2. Additional Visualisations

Fig 10 shows the distribution of triplets in the  $(d_0, d_1)$  plane for the training set used to find  $\hat{P}(d_0, d_1)$  from the CLIC dataset. Note that the triplets shown vary in number of judgements  $M_t = \{1, 2\}$ , and when training the triplets are treated as binary judgements ( $M = 1$ ) on  $M_t$  identical triplets.

We also show the surface of the binomial parameter  $\hat{P}(d_0, d_1)$  in the  $(d_0, d_1)$  plane estimated from the CLIC training set for both the proposed density estimation method and neural network.

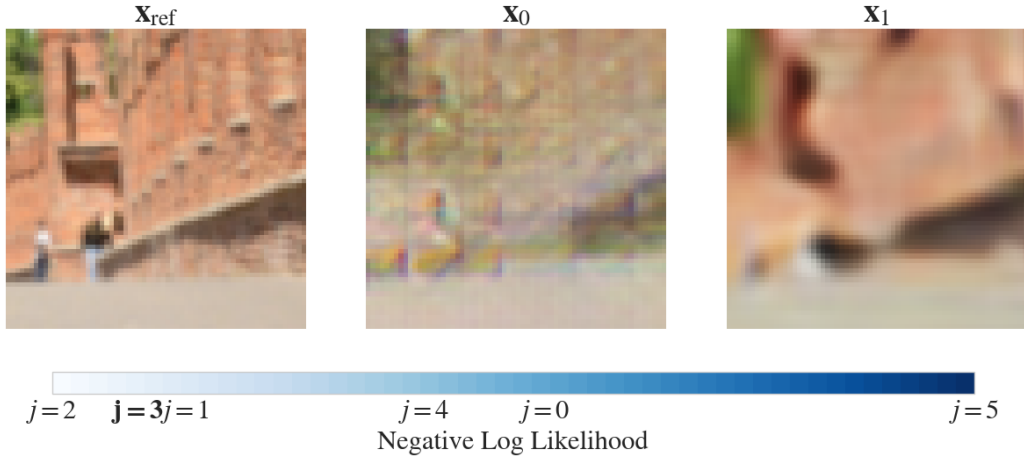


Figure 8: Example of valuating the negative log-likelihood  $j = [0, 5]$  according to DISTS for a triplet from the BAPPS test set where both images  $\{x_0, x_1\}$  are far from the reference  $x_{\text{ref}}$ . White is more likely and blue is less likely.

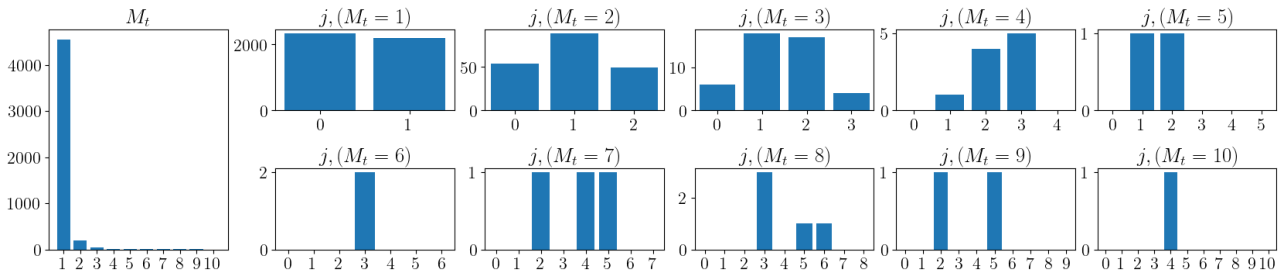


Figure 9: Distribution of number of judgements  $M_t$ , and resulting judgements  $j$  for the CLIC data used for evaluation.

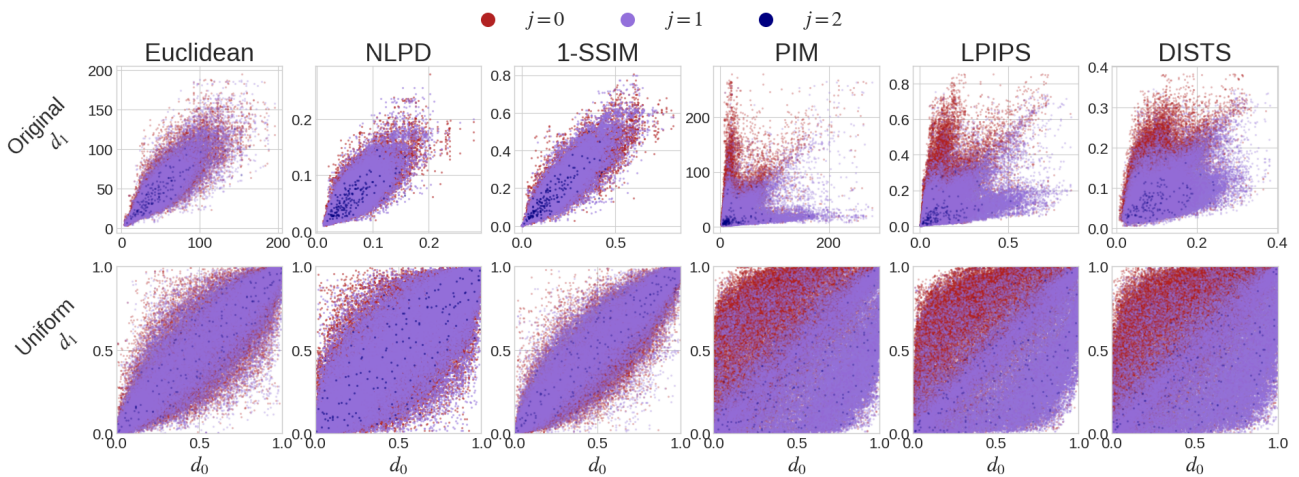


Figure 10: Candidate distances in their original space (top row) and uniformised (bottom row). Shown are the training samples from the CLIC dataset and the colour indicates the judgement assigned to the triplet according to  $\{1, 2\}$  observers. The points in this plot have a varying number of observers  $M$ .

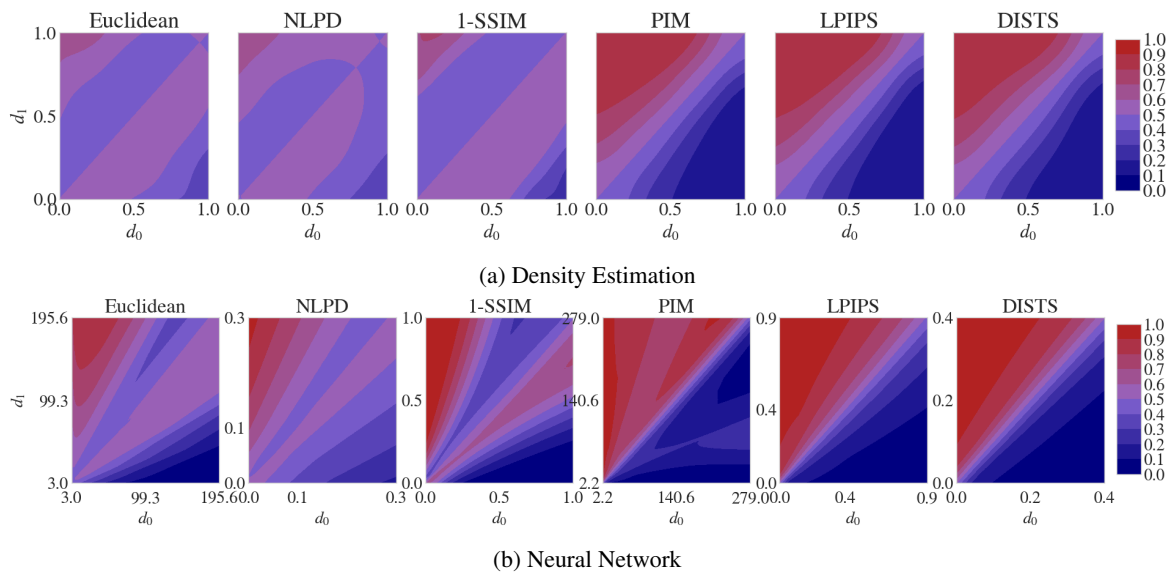


Figure 11: Binomial parameter  $P$  estimated from the training set of CLIC, for different candidate distances for (a) Density estimation and (b) Neural network